High Resolution Computed Tomography Inspection of Components Uncovers Root Causes of Vexing Failure Mysteries

Michael R. Johnson*

Abstract

During testing of actuators for fight programs, failures have occurred that required closure with an understanding of the root cause of the failure. For some InSight project actuators, intermittent changes of the winding resistance of the motors during temperature changes was extremely baffling. It was critical to determine the cause of the intermittent characteristic because the actuators were stock from a previous program and the company that provided the motors was no longer in business. Using an X-Ray Computed-Tomography (CT) method, the exact source of the intermittent failure was determined and completely understood – at dimensions of less than 20 microns. In another case, after the completion of an actuator's life-test-to-failure, inspection was required to determine the source of the failure. The size of the actuator (10 mm diameter) required destructive means to get to the interior of the actuator for inspection, risking the loss of the source of the failure. Using CT imaging, the exact source of the failure was determined.

Introduction

Computed Tomography X-Ray inspection is a process that uses hundreds to thousands of X-ray images to assemble a finely detailed three-dimensional computer model of the object under inspection. By taking each image from a different location and angle around the perimeter of the object, a three-dimensional volumetric model can be created from the individual scans. This model can then be viewed, rotated, sectioned, and magnified in the same way as a computer design model of the object. By rotating, sectioning, and magnifying the scanned model, details of the actual assembled components within the assembly can be detected and measured. These measurements and views allow the illumination of anomalies within the assembly that may otherwise be undetectable.

Two anomaly investigations are discussed that demonstrate the power of the X-Ray Computed Tomography inspection method. One case allowed the detection of failure points that were not visible even though the hardware could be safely disassembled and inspected directly. The second case allowed the determination of the failure cause with a hardware assembly that could not be disassembled without destructive means. The destructive disassembly required caused significant concern that the root cause would be lost in the process of disassembly. The use of the Computed Tomography method allowed the determination of the failure source and in-situ measurements of the effects of the failure could be made to fully demonstrate the extent of the failure cause.

The two cases described are:

1. Winding failures of brushed motors for the Instrument Deployment Arm on the Insight Project
2. Brushless Actuator Life Test failure of a 10mm diameter device for the Mars 2020 project

* Jet Propulsion Laboratory, California Institute of Technology, Pasadena, California

Proceedings of the 44th Aerospace Mechanisms Symposium, Jet Propulsion Laboratory, May 16-18, 2018

Insight Instrument Deployment Arm (IDA) Motor Winding Anomaly

Instrument Deployment Arm (IDA) Hardware Description

The IDA for the InSight Project is utilized to place instruments onto the Mars surface after landing of the spacecraft. A rendering of the lander on the surface of Mars is shown in Figure 1. The IDA is identified in the picture and has four axes of motion that utilize the motors under investigation.

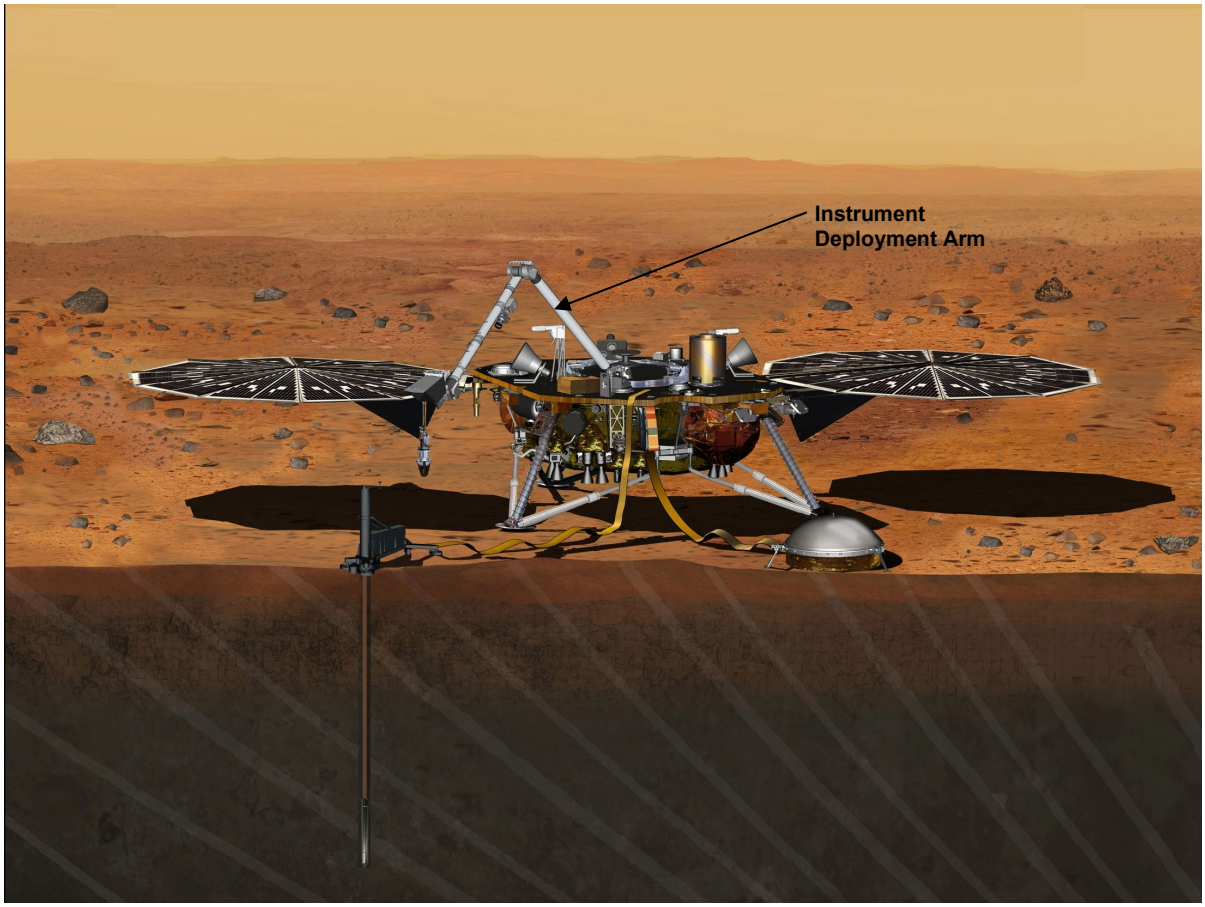

Figure 1. InSight Lander Shown on the Surface of Mars

The IDA is exposed directly to the environment of Mars and experiences large changes in temperature from day to night. This thermal cycling can have deleterious effects on assemblies composed of materials with different coefficients of thermal expansion. To demonstrate the capability of the motors, a thermal cycle test was performed on three units. To establish design margin, the number of test thermal cycles is much larger than the quantity of cycles during the mission. This type of thermal cycle testing is considered a qualification test and the hardware is not flight worthy after going through the testing. For brushed motor assemblies, the adhesively bonded windings on the rotor and the winding terminations to the commutator are the primary thermal cycle sensitive items. There are also the bonds between the magnets and the housing and other ancillary areas that are also stressed during the thermal cycle testing. One of the three test motors, serial number 041 is shown in Figures 2, 3, and 4.

Figure 2. Motor Serial Number 041
Motor Diameter is 30 mm

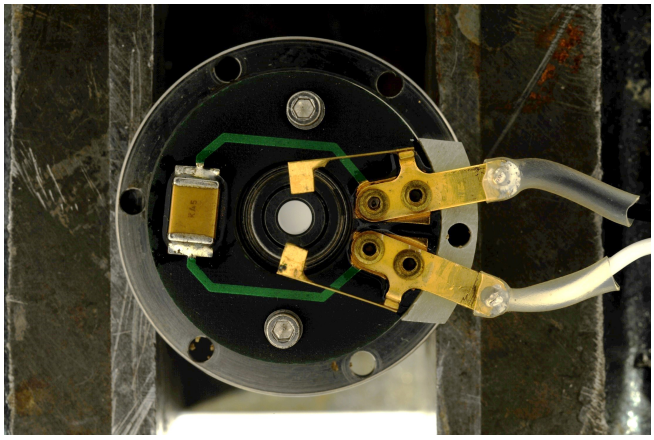

Figure 3. Brush Assembly

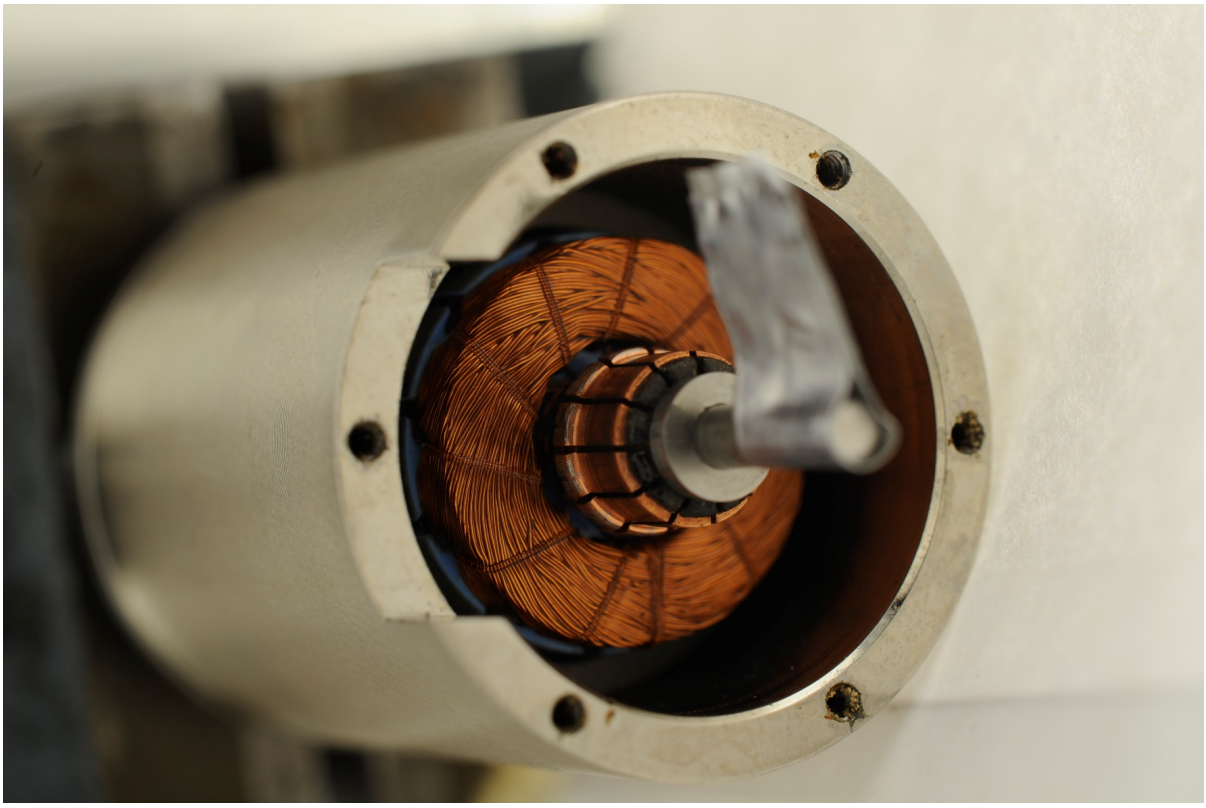

Figure 4. View of the Shaft End with the Commutator and Winding Terminations Shown

Thermal Cycle Test Setup

Three motors were selected for thermal cycle testing and placed in the thermal chamber. The motors are not rotated during the thermal cycle testing to enable accurate measurements of the winding resistance. The instrumentation was connected to read the winding resistance of the motors as shown in Figure 5 while the temperature was cycled from hot to cold. The temperature of various locations on the motor assemblies and voltage drop across the windings (resistance) was recorded continuously during the test. The resistance of the windings varies directly with the temperature of the test article. The expected appearance of the recorded data for the windings would show the resistance of the windings rising and falling smoothly with the temperature of motor as shown in Figure 6.

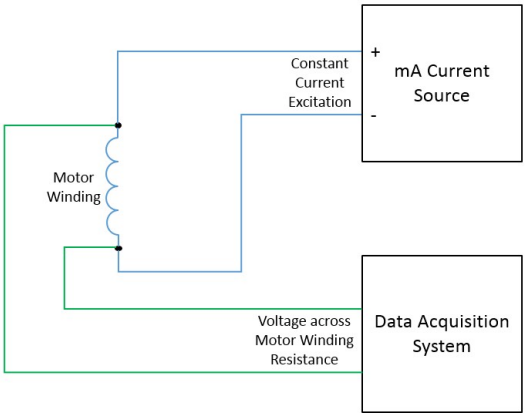

Figure 5. Test Instrumentation

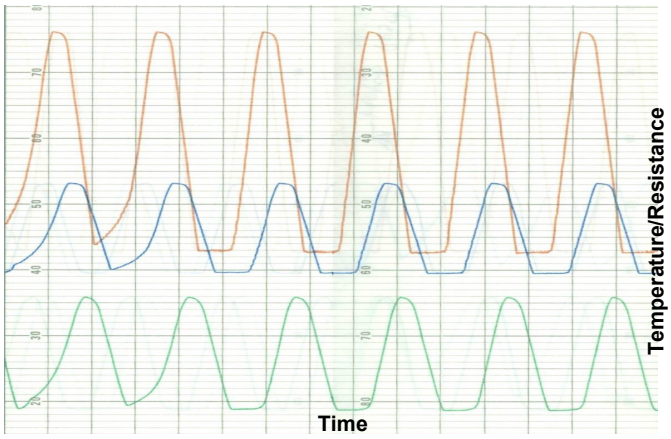

Figure 6. Typical Shape of Winding Resistance versus Time Showing Smooth Variation with Temperature Cycles

The Anomaly Appears

The resistance recorded for one of the three motors looked mostly as expected for the first few thermal cycles of the testing. Some measurement noise was present in the data traces. Two of the motors, however, did not produce the results expected. The traces instead appeared as in Figure 7. The blue curve is the temperature and the grey, orange, and yellow curves are the motor winding resistances.

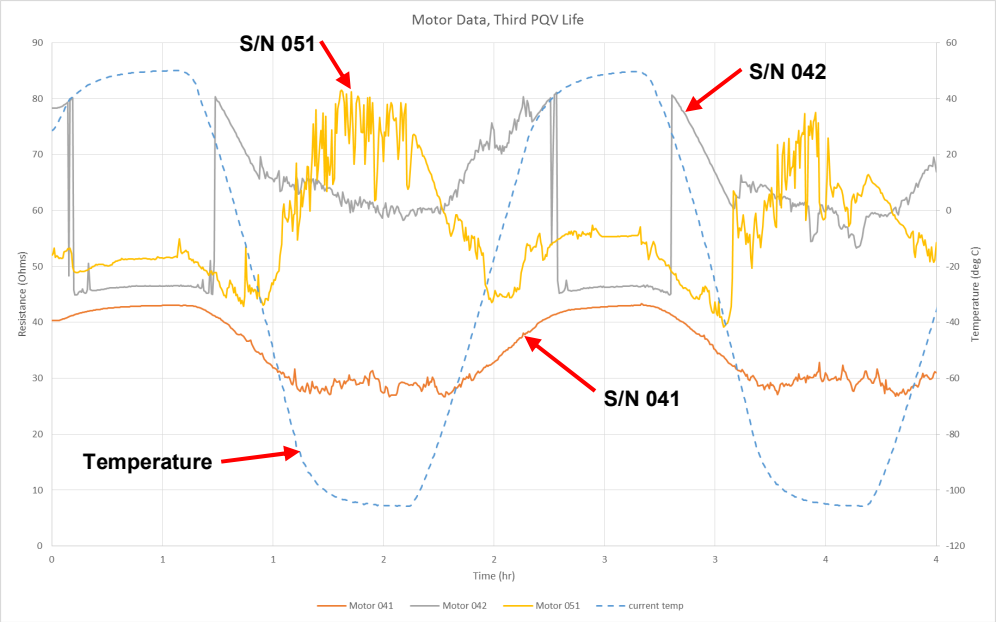

Figure 7. Motor Resistance and Temperature versus Time Plot for Cycle #3

The orange curve is motor serial number 041, the grey curve is motor serial number 042, and the yellow curve is motor serial number 051. The winding resistance of all of the motors shows electrical noise during the region of low temperature dwells. The orange motor data performed as expected. The noise within the data was unexpected and a little troubling, but the most significant feature of the grey and yellow curves is the sudden change in apparent resistance of the windings during the transitions to and from the cold temperatures. During the cold transition, the winding resistance should smoothly lower and at no time should it indicate an increase or sudden jump up in resistance. After 38 temperature cycles, serial number 041 adopted the same signature as the other two motors, with a sudden increase of winding resistance as the temperature was lowered through the cold portion of the cycle (see Figure 8).

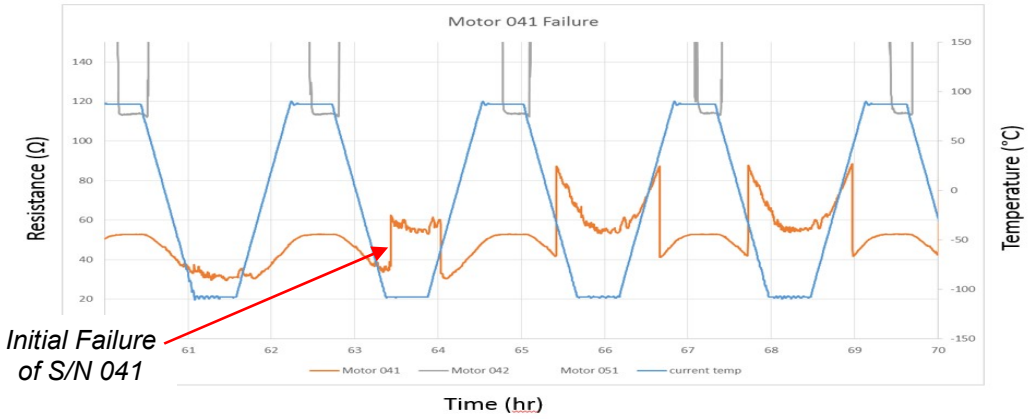

Figure 8. Failure of Serial Number 041 at Temperature Cycle #38

To determine the source of the strange increases in resistance, the motor was disassembled and inspected at high magnification. The motor windings are bonded together and to the rotor core laminations with an epoxy. During visual inspection under high magnification, some indications of cracks in the epoxy were detected. The images do not indicate if the cracks are the source of the winding resistance anomalies, but they are certainly potential locations for trouble. Some of the images taken are shown in Figures 9 and 10. The cracks indicated in the images were not present in the motor winding epoxy prior to the thermal cycle testing.

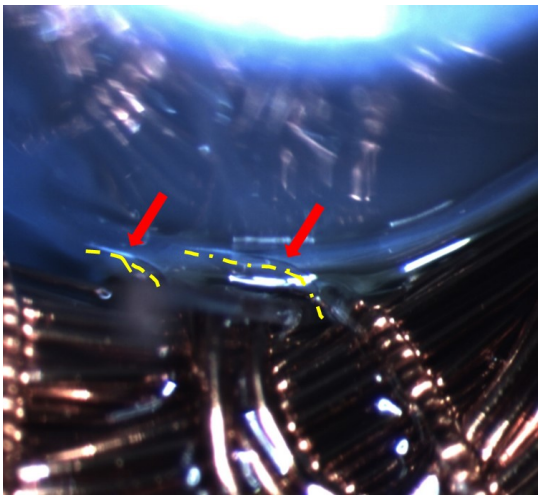

Figure 9. Winding/Rotor Epoxy Cracks Indicated by Lines and Arrows

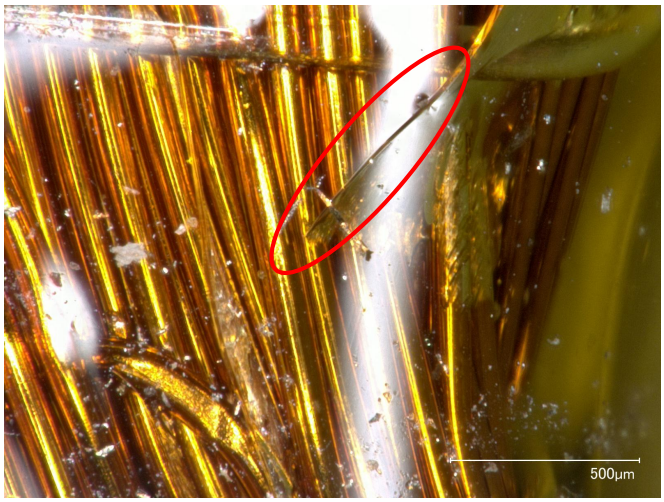

Figure 10. Winding/Rotor Epoxy - Crack in Epoxy Shown in Red Oval

None of the inspection methods had indicated the actual source of the resistance changes. Some locations were implicated by the presence of cracks in the epoxy coating, but none of them showed any signs of a feature that would cause an increase in resistance as the temperature is reduced during the cold temperature portion of the thermal cycles. The solder joints at the commutator were inspected as well and, while some of the joints had workmanship issues, none of the connections showed any type of failure that would support the test data. The brush block/commutator/shaft assembly was X-Ray inspected while installed in the motor and the brush springs (cantilever arms) showed a proper preload on the brushes as indicated by the deflection of the spring arm (see Figure 11).

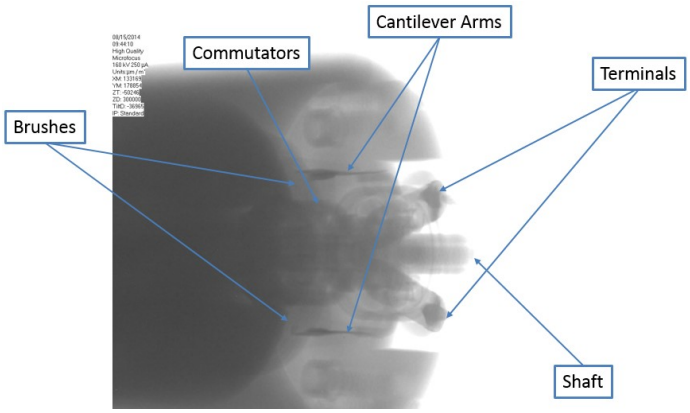

Figure 11. X-Ray Image of the Brush/Commutator Assembly

The next inspection method used was a Computed Tomography X-Ray Three-Dimensional inspection technique, or "CT Scan". The process uses x-rays to illuminate the component being measured and captures the image on a line array detector. The item (or source/detector pair) is then moved slightly and another image taken. This is repeated thousands of times and the images are then consolidated into a single three-dimensional computer model of the item being scanned. The model that is produced from the scanning of the motor assembly is a 3-D computer model that can be rotated and sectioned for very fine detailed inspection.

Overall CT Scan views of the rotor assembly are shown in Figures 12, 13, and 14. Figure 12 shows the rotor assembly with the individual winding wires clearly visible. Figure 13 is a cross-section of the rotor with one slot on the rotor exposed and the wires within the slot visible in fine detail. Figure 13 is a view of the brush assembly end of the shaft with the brushes and cantilever arms clearly visible.

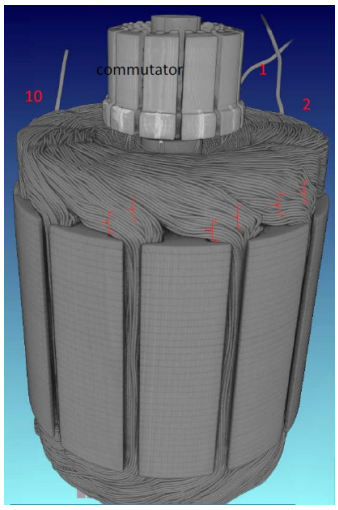

Figure 12. Rotor Assembly

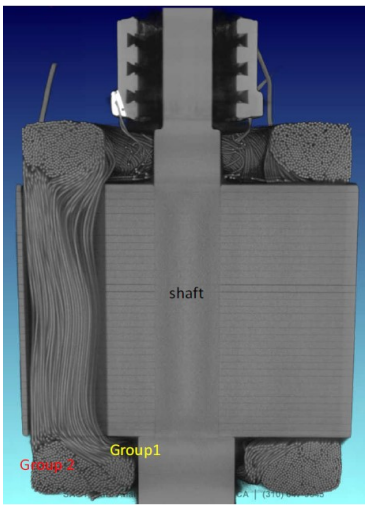

Figure 13. Section of Rotor Showing Wires in the Slot

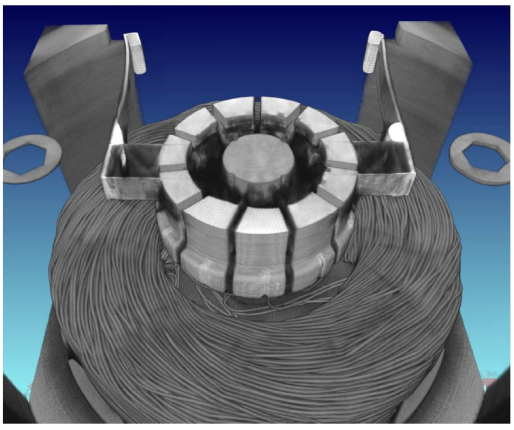

Figure 14. Brushes, Commutator, and Cantilever Arms

The CT Scan inspection method provides high resolution three-dimensional computer models that can be interrogated in locations within the assembly that are otherwise not possible to inspect. Since no disassembly is required, the in-situ state of all components can be viewed. Addtionally, any failure condition that may be disturbed by disassembly can be captured without risk of losing the failure evidence in the process of removing intervening material.

Close inspection of the CT Scan model revealed the source of the winding failures to be coincident with the crack sites of the epoxy located on the opposite end of the rotor from the commutator assembly and winding wire terminations. Figure 15 shows a close-up view of the end of the rotor where the wires exit the slots and there is indication of damage to the winding wires, identified by the red arrows. Focusing on the areas of apparent damage, the culprit is finally found to be broken winding wires at the exact locations of the epoxy cracks. The wire can be seen to have necked down prior to failing, indicating a tensile failure.

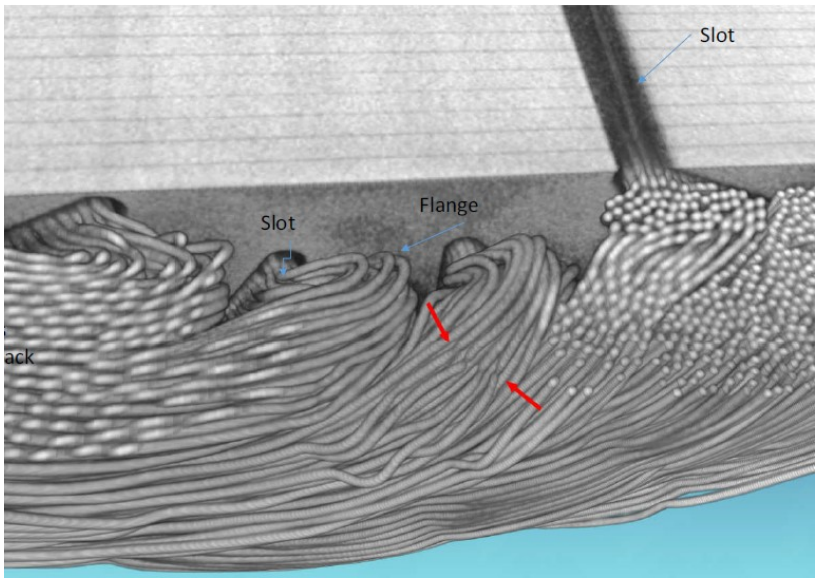

Figure 15. Magnified View of the CT Scan Model Showing the End Turns and the Slots in the Rotor Laminations

Further investigation of other epoxy crack locations revealed several failed wires and many stretched wires with necked down cross-sections. The necking would account for resistance changes in the first few cycles after the epoxy crack propagated to the location of the wires. The sudden increases of winding resistance in the test data were the result of several broken regions moving back together as the temperature was raised. While the winding resistance might have appeared nominal at a higher temperature, the winding wire damage points would certainly not have supported a high enough load current to produce the required torque output from the motor in the IDA application.

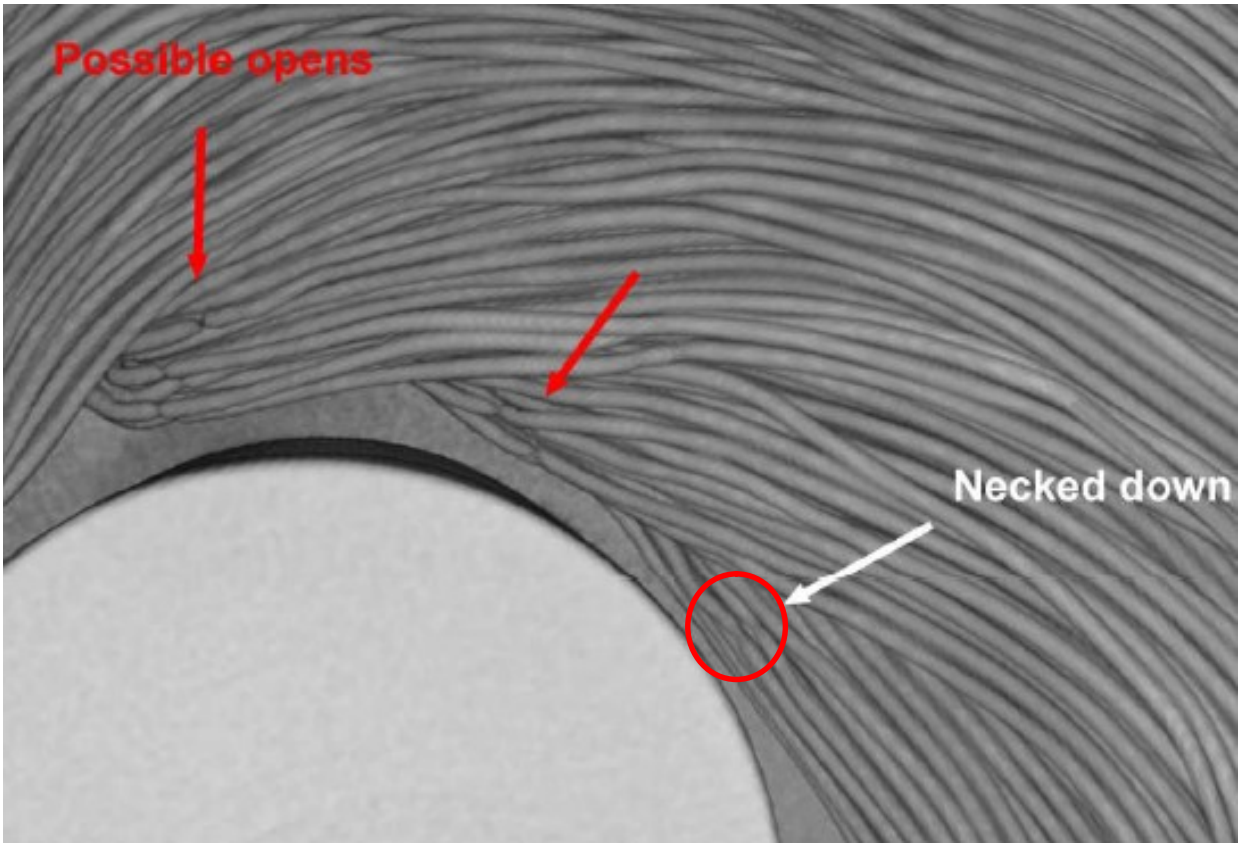

Fogure 16. View Showing Several Locations of Failed Wires. The Necking Down of the Breaks Indicates Tensile Failures. The Wire Breaks Follow the Cracks in the Epoxy Coating. The wire diameter in the image is 80 microns.

10 mm Motor/Gearbox Life-Test-to-Failure Determination of Failure Source

10 mm Motor/Gearbox Application Hardware Description

The 10 mm motor and gearbox assembly is comprised of a three-phase brushless dc motor attached to a 16:1 reduction ratio planetary gearbox. The motor has ball bearings on the rotor and the gearbox planet gears use plane bearings. The gearbox is lubricated with Bray grease, type 601. There are two preloaded ball bearings on the output of the gearbox to provide a moment carrying capacity for offset loads on the output shaft. The face width of the planet gears is approximately one millimeter and the ring gear is made from bronze.

The 10 mm actuator drives the filter wheel of the Mast cameras on the Curiosity rover operating on the surface of Mars. The actuator has a pinion gear attached to the output shaft and is mounted into a housing that contains the larger filter wheel for the camera. The pinion gear on the actuator output drives the filter wheel directly with a gear mesh on the outside diameter of the filter wheel disc. The motor is operated as a stepper motor in this application, so no rotor position sensors are mounted within the motor housing. There is a magnetic detent wheel attached to the back of the rotor to provide the necessary magnetic detent for proper stepper motor function. The filter wheel assembly is shown in Figure 17. Magnets on the filter wheel itself are sensed with hall sensors in the housing to confirm filter position during operation of the mechanism.

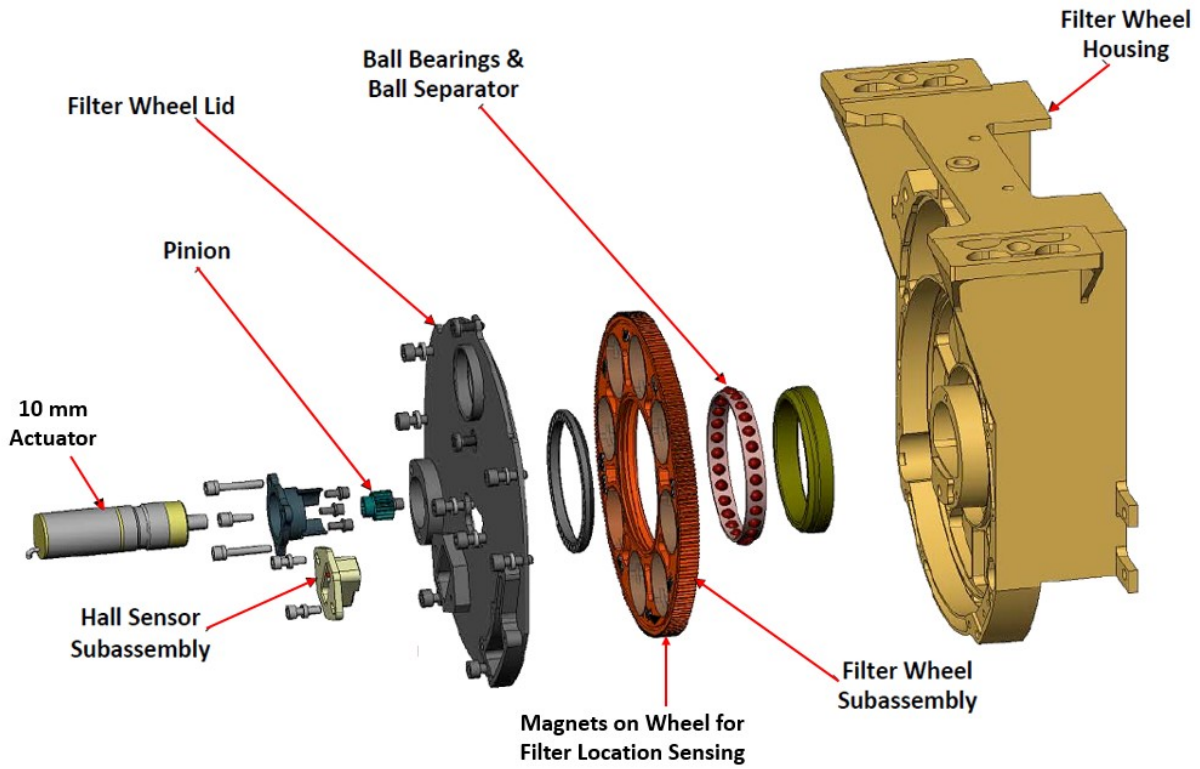

Figure 17. Filter Wheel Assembly Application of the 10 mm Actuator

Life Test Setup

Two Filter Wheel Assemblies were used on the Curiosity Rover mission. Two Filter Wheel Assemblies are also being put in the new camera build for the Mars 2020 mission. Since the Mars 2020 mission is a longer duration than the Curiosity mission, the life test that was performed on the Filter Wheel mechanism for the Curiosity mission was not adequate for the newer mission requirements. The life test Filter Wheel Assembly from the Curiosity hardware build was resurrected and placed into a life test to understand if any fundamental limitations of the hardware design existed that might affect its use for the Mars 2020 misision. The test configuration placed the Filter Wheel assembly on a test bench with the actuator in the

horizontal position. This was done to minimize the possible effect of the presence of a gravity vector. In the application on Mars, the actuators are in the horizontal position as well. The actuator was operated using a motor driver that provided a pulse width modulated motor coil drive current. The pulse width modulation was to set a current level for the motor that was less than the maximum possible winding current at the applied drive voltage. The current limit is used for the flight unit drive and allows limiting of the output torque of the motor. The setup of the test equipment for the life test is diagrammed in Figure 18. The Stepper Motor Driver operates the motor and the actuator rotates the Filter Wheel Assembly. The magnets on the filter wheel provide indications of filter position back to the comparator while the wheel is turning. The number of steps between filters is a known value. The comparator checks the number of steps it took to move between filters to the known number of steps between filters. If the step count does not match the predicted value within a couple of steps, the comparator declares missed steps.

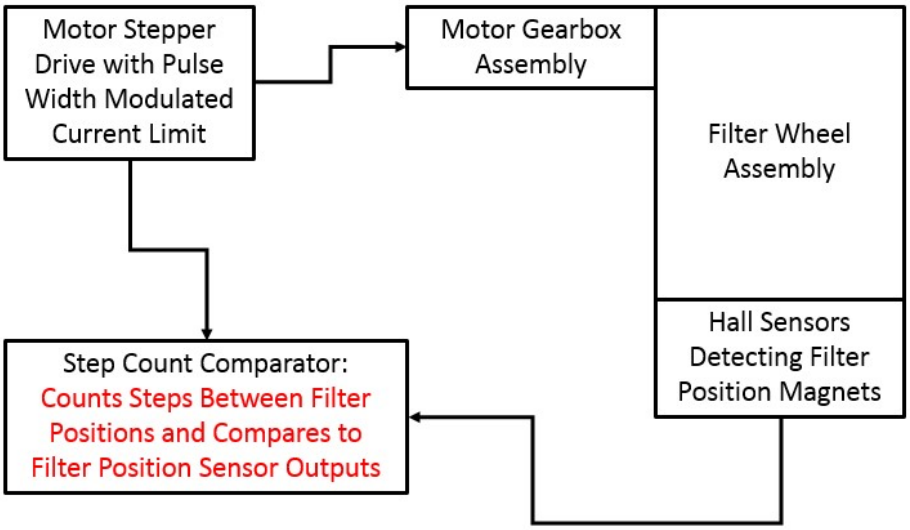

Figure 18. Block Diagram of the Filter Wheel Assembly Life Test Setup

For the life testing, the motor current limit was determined by reducing the limit until the operating motor started missing steps. This is the threshold limit for the operation of the stepper motor at the applied torque load. The life test was started with the motor driver current limit set to a value of 20% of the maximum drive capability, which was a little above the drive at which the motor missed steps. The motor was operated continuously and the number of steps between filter positions were checked until the motor skipped steps. The motor drive current limit was then raised to 45% of the maximum, which was the value needed to reliably rotate the actuator without missing steps at the higher torque load. The test was continued until the motor started missing steps again. The third time the motor drive output was raised to 100% of the output capability. The test was continued until the motor started skipping steps once more. Since the maximum drive capability was reached, the test was terminated at that time. The total number of output revolutions demonstrated was over 14 times the required life for the Mars 2020 mission, indicating a high level of robustness of the Filter Wheel Assembly design for the application.

Determination of the Cause of the Failure to Rotate

The final operation to perform after the completion of the life testing phase was to determine the cause of the Filter Wheel Assembly's failure to rotate reliably. The first step in this process was to remove the actuator from the filter Wheel Assembly and operate the actuator alone. The actuator would still not rotate reliably separated from the Filter Wheel Assembly. This indicated that the actuator was the source of the failure to rotate reliably for the entire mechanism. The actuator was placed into a Fein focus real-time X-ray machine and inspected for possible causes of the failure. Figures 19 and 20 show images from the x-ray machine.

Figure 19. X-Ray Image Showing the Gearbox Section of the Actuator. Output Ball Bearings are at the Top of the Image and the Front Motor Bearing is at the Bottom

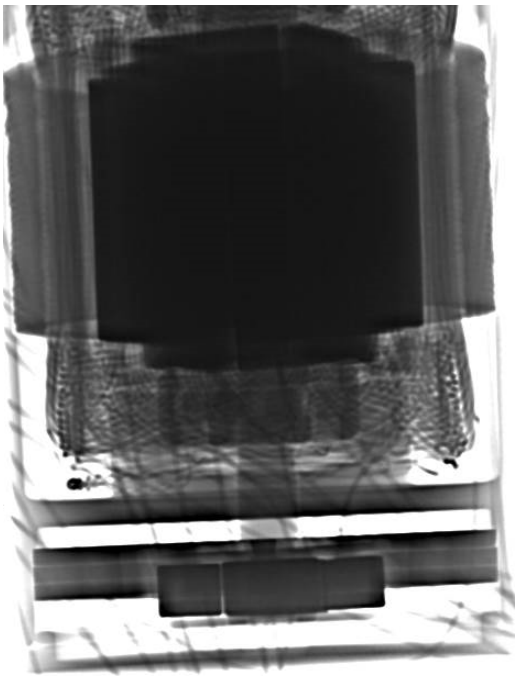

Figure 20. X-Ray Image Showing the Detent Magnet Section of the Motor Assembly. Magnets are on the Rotor and the Teeth are on the Stator

From the x-ray images there is no apparent problem within the actuator at all. The gearbox looks to be in good shape, the bearings at the gearbox output show no indication of extreme wear or debris, the motor bearings do not show any sign of wear or debris, and the motor windings show no indication of being damaged. The failure mechanism needed to be consistent with a wear phenomenon since the test required a slowly increasing drive current to keep the mechanism operating properly. This would indicate an increasing load torque as opposed to a sudden change. The only item detected with the x-ray images was the offset of the detent wheel from the detent stator. This appeared to be a manufacturing defect since it would not explain a slowly increasing load torque.

The Culprit is Exposed!

The next possible inspection method involved opening up the gearbox and motor to directly inspect the components for wear and debris. The problem with this method is that the 10 mm actuator is not built to be disassembled. The component items are bonded together and machining would be required to separate the parts. There was a significant concern that a machining process may dislodge the source of the drag torque and the failure would be permanently lost. To eliminate this concern, the CT Scanning method was employed. The volume of the actuator is small and the resolution of the machine is a fixed value for the scan volume. If the volume size is made smaller, the image dimensional resolution is increased. The actuator was CT Scanned and the model was queried to determine the source of the drag torque. The gearbox was the suspected guilty party, so it was inspected in detail first.

Figure 21 shows the overall view of the motor and gearbox assembly for the 10 mm actuator. The CT Scan detailed computer model allows the cross-sectioning of the image so internal components can be inspected. In this actuator, the planetary gear faces are one millimeter wide. The bright portions of the image are the permanent magnets due to their high density. Figures 22 and 23 show the planetary gear stages in a cross-section of the computer model at each stage location. No debris is visible and no wear

of the gear tooth form is evident from the image. The gear teeth and tooth form look as if there is no wear at all. The input to the first stage of the planetary gears had been through 258 million revolutions at this point.

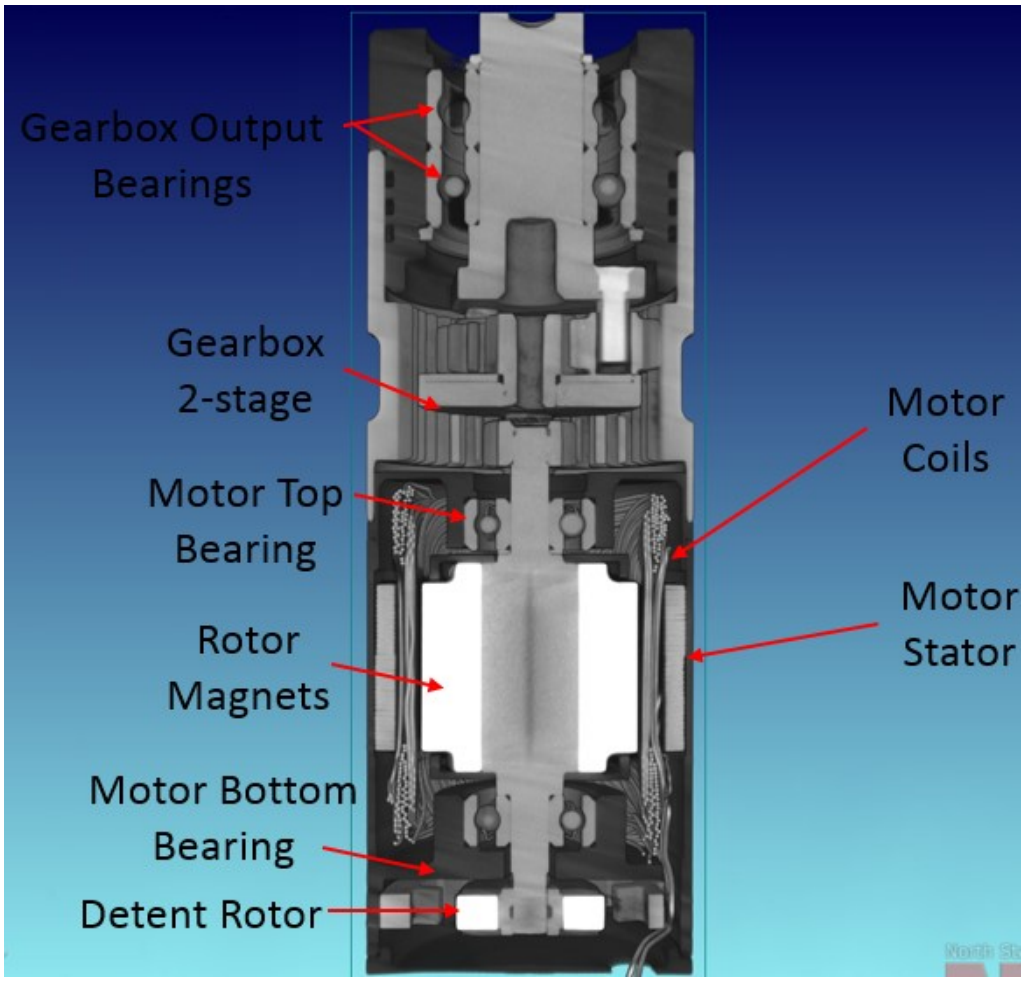

Figure 21. Overall Image Cross-Section of the 10 mm Actuator Assembly

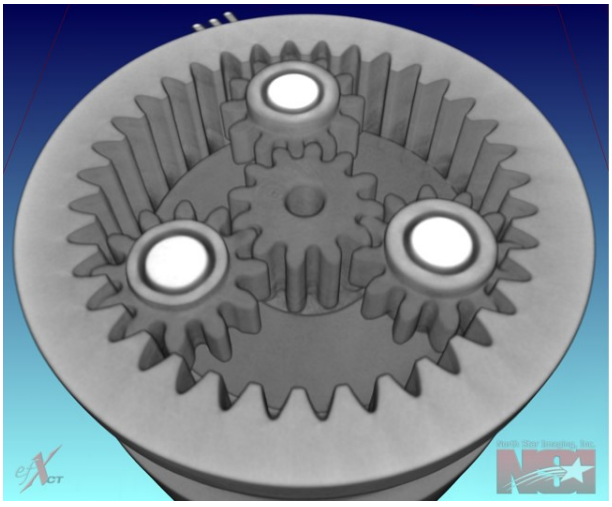

Figure 22. Second Planetary Gear Stage

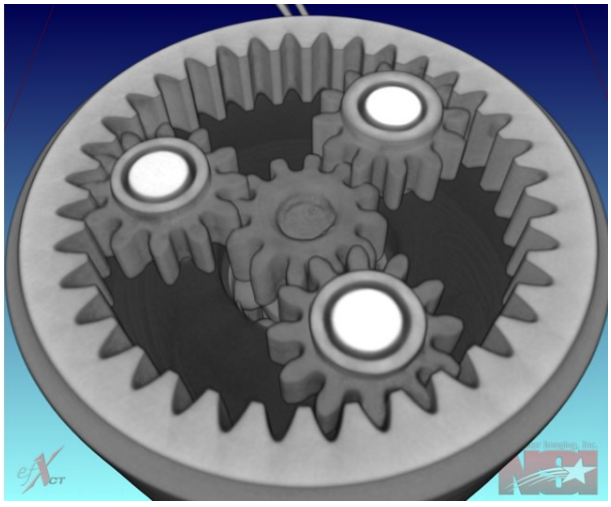

Figure 23. First Planetary Gear Stage with the Motor Pinion at the Center

The view of the first stage of the planetary gears seemed to show an offset of the pinion gear toward the motor. This necessitated an inspection of the front motor bearing. Looking at a section of the model from the side in Figure 24 shows that the motor bearing appears to have shifted downward in the image and the motor pinion gear has done the same. Scrutinizing the bearing assembly itself shows no unusual wear or debris. All other elements of the motor assembly in this region seem fine.

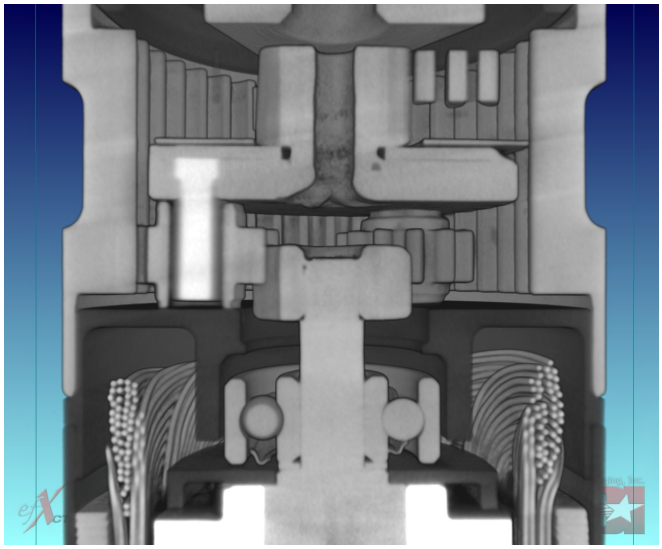

Figure 24. Side View of the First Planetary Gear Stage with the Motor Pinion at the Center. The Bearing is Displaced Downward in the Image

The offset of the rotor was a mystery and required further investigations. Looking at an isometric view of the section of the motor through the shaft at the front motor bearing did not expose anything unusual. Figure 25 shows the view with the front motor bearing fully intact with no significant wear or debris.

Moving down to the rotor detent assembly, the detent magnets are positioned properly within the inside diameter of the detent stator and no anomalous behavior appears at this location. Figure 26 shows this region of the motor assembly with no visible indication of a torque drag anomaly.

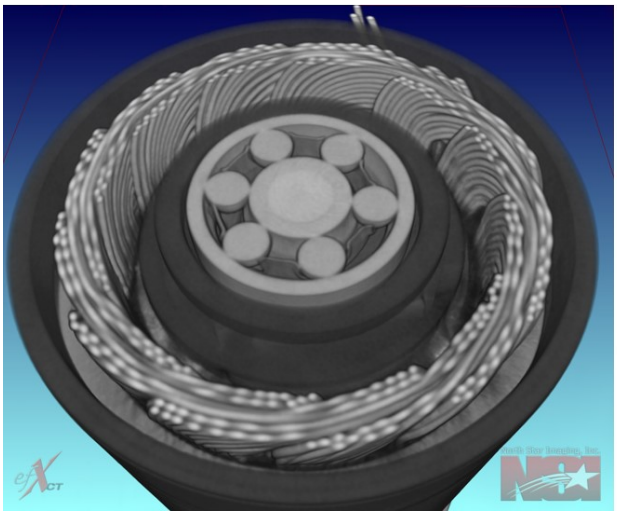

Figure 25. Front Motor Bearing Closest to the Gearbox Input

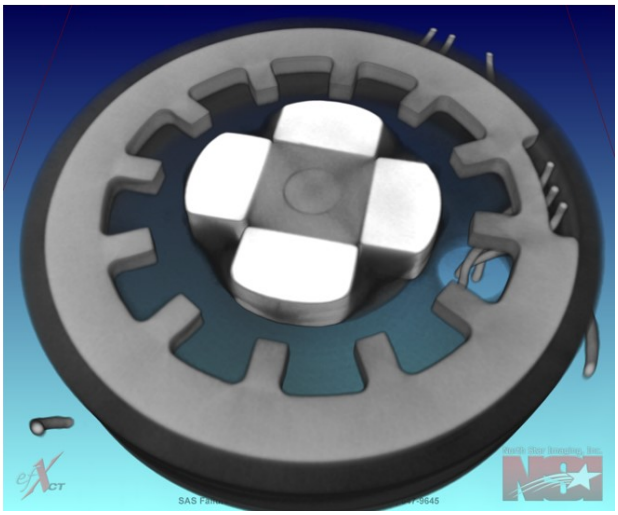

Figure 26. Detent Rotor and Stator

Inspecting the CT Scan model further finally showed a source of the drag. The rear motor bearing is shown in Figure 27 and the ball separator is missing. The balls have moved within the bearing assembly to a position where they have jammed and the bearing will not rotate. While the jammed bearing appeared to be the guilty party, it could not explain an increasing torque load over time. The problem with the bearing jam being the source of the drag is the jam does not allow the bearing to rotate. This should have stopped the actuator suddenly and not in the manner of a slowly increasing drag torque.

Closer inspection provided the needed clues to the solution. The shaft in the bore of the bearing in figure 27 appears to be smaller than the bore. Figures 28 and 29 show a side-by-side comparison of the end of the motor with an as-built beginning of life motor on the left and the failed life test motor on the right.

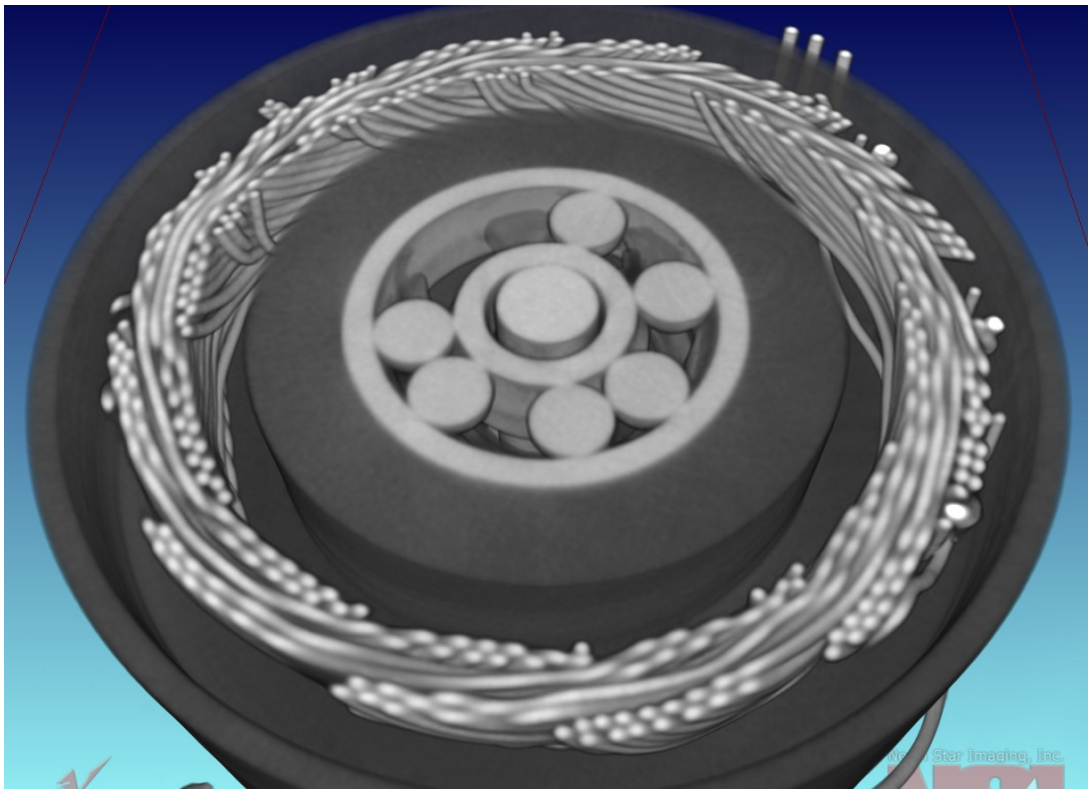

Figure 27. View of the Rear Motor Bearing Showing the Balls Have Displaced Around the Circumference of the Bearing Races to a Jamming Position. This Makes the Bearing Unable to Rotate at All.

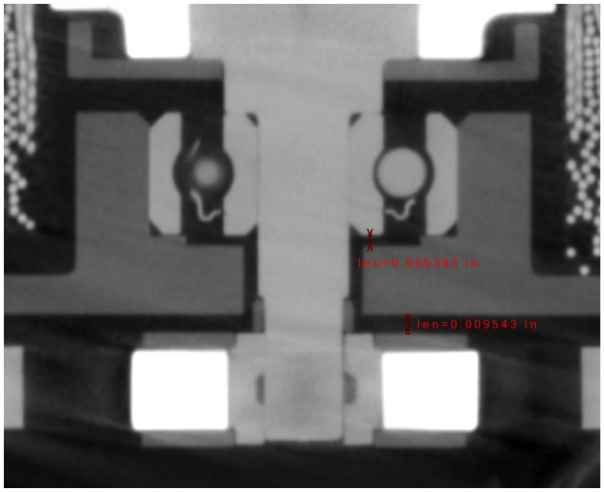

Figure 28. Healthy Motor at the Beginning of Life Showing Bearing Placement and Shaft Fit. The measurements in the images are in inches (0.0095 in = 241 microns)

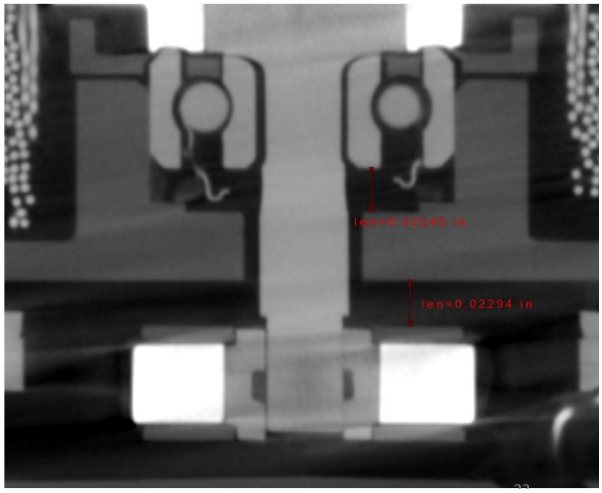

Figure 29. Life Test Motor Showing Shaft Wear and the Bearing Having Moved Toward the Rotor. The Ball Retainer is Seen Located Under the Bearing Assembly. (0.0229 in = 582 microns)

Figure 30 shows a close-up of the rear ball bearing and where it is dragging on the rotor (from Figure 29). The bearing has cut through the magnet end cap (aluminum) and started cutting into the magnet material. The rotor diameter has also worn significantly smaller than the bearing bore. The root cause of the failure

was the bearing seizing and stopping rotation. This was followed by the rotor shaft rotating in the bore of the bearing inner race. Since a stepper motor does not provide current feedback that is related to load torque, the jamming of the ball bearing was not detected. This event was missed because the motor rotor was assembled with a small clearance to the ball bearing bore and that allowed the rotor to rotate within the bore of the bearing. This motion started the wearing of the rear section until too many components were dragging on each other.

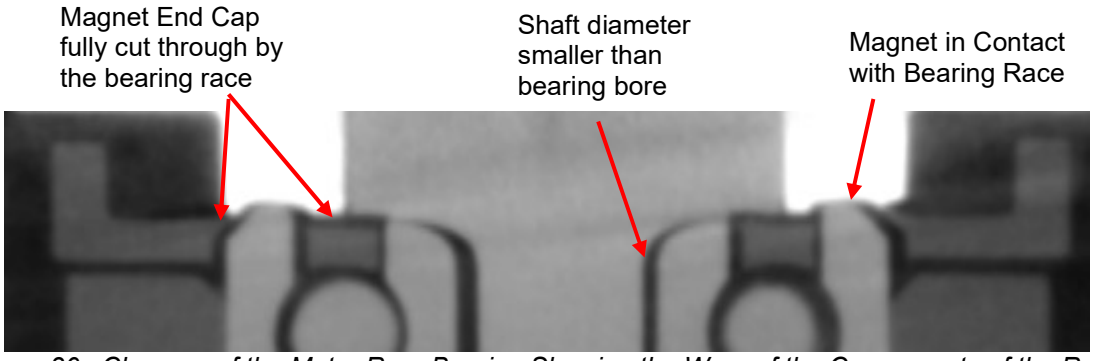

Figure 30. Close-up of the Motor Rear Bearing Showing the Wear of the Components of the Rotor

An interesting point is the components all have a thrust load on them that draws them toward the rotor. This thrust load is from the magnet flux at the end of the magnets. This is often not a significant player in the performance of a motor, but the thrust load is enough to draw the component into the rotor such that, if there is sliding contact, significant wear can occur.

Conclusions and Lessons Learned

The CT Scan inspection method is extremely powerful in diagnosing failures in mechanical assemblies where access to the suspect regions of the hardware is very difficult or impossible. It is also great to use where the accessing of the internals has the risk of losing the failure. Since the most important tenet of troubleshooting is to NEVER LOSE THE FAILURE, the CT Scanning method is a fantastic resource.

Additionally, thermal cycling of motor windings for extreme cases is paramount to having confidence in mission success. Continuous monitoring during the temperature cycling of the item being tested is critical since the failure may not be present at room temperature, as was the case with the InSight IDA motors.

Lastly, making the rotor free to rotate within the motor bearing bores, if possible, provides a robust and graceful degradation path for actuator motors. This is especially important at the lowest torque location within the mechanism – the motor rotor.

Acknowledgements

This work was performed at the Jet Propulsion Laboratory, California Institute of Technology, under a contract with the National Aeronautics and Space Administration. Reference herein to any specific commercial product, process, or service by trade name, trademark, manufacturer, or otherwise does not constitute or imply its endorsement by the United States Government or the Jet Propulsion Laboratory, Pasadena, California. Government sponsorship acknowledged.

The author wishes to acknowledge the great contributions provided by the InSight failure analysis team and the associated review boards in uncovering the root cause of the winding anomalies. On the 10 mm Actuator failure analysis effort, Malin Space Science Systems performed the life test and provided invaluable information and access to the Filter Wheel Assembly actuator at the conclusion of the life test. Malin Space Science Systems facility is located in San Diego, California.